Korean Journal of Radiology

Imaging Features of Primary Tumors and Metastatic Patterns of the Extraskeletal Ewing Sarcoma Family of Tumors in Adults: A 17-Year Experience at a Single Institution

Jimi Huh, MD[1], Kyung Won Kim, MD, PhD[1], Seong Joon Park, MD[2], Hyoung Jung Kim, MD[1], Jong Seok Lee, MD[1], Hyun Kwon Ha, MD[1], Sree Harsha Tirumani, MD[3], Nikhil H. Ramaiya, MD[3]

Departments of [1]Radiology and [2]Oncology, Asan Medical Center, University of Ulsan College of Medicine, Seoul 138-736, Korea; [3]Department of Imaging, Dana-Farber Cancer Institute, Brigham and Women's Hospital, Harvard Medical School, Boston, MA 02115, USA

Objective: To comprehensively analyze the spectrum of imaging features of the primary tumors and metastatic patterns of the Extraskeletal Ewing sarcoma family of tumors (EES) in adults.

Materials and Methods: We performed a computerized search of our hospital's data-warehouse from 1996 to 2013 using codes for Ewing sarcoma and primitive neuroectodermal tumors as well as the demographic code for ≥ 18 years of age. We selected subjects who were histologically confirmed to have Ewing sarcoma of extraskeletal origin. Imaging features of the primary tumor and metastatic disease were evaluated for lesion location, size, enhancement pattern, necrosis, margin, and invasion of adjacent organs.

Results: Among the 70 patients (mean age, 35.8 ± 15.6 years; range, 18–67 years) included in our study, primary tumors of EES occurred in the soft tissue and extremities (n = 20), abdomen and pelvis (n = 18), thorax (n = 14), paravertebral space (n = 8), head and neck (n = 6), and an unknown primary site (n = 4). Most primary tumors manifested as large and bulky soft-tissue masses (mean size, 9.0 cm; range, 1.3–23.0 cm), frequently invading adjacent organs (45.6%) and showed heterogeneous enhancement (73.7%), a well-defined (66.7%) margin, and partial necrosis/cystic degeneration (81.9%). Notably, 29 patients had metastatic disease detected at their initial diagnosis. The most frequent site of metastasis was lymph nodes (75.9%), followed by bone (31.0%), lung (20.7%), abdominal solid organs (13.8%), peritoneum (13.8%), pleura (6.9%), and brain (3.4%).

Conclusion: Primary tumors of EES can occur anywhere and mostly manifest as large and bulky, soft-tissue masses. Lymph nodes are the most frequent metastasis sites.

Index terms: *Ewing sarcoma family of tumors; Extraskeletal Ewing sarcoma; Computed tomography; Imaging*

Corresponding author: Kyung Won Kim, MD, PhD, Department of Radiology, Asan Medical Center, University of Ulsan College of Medicine, 88 Olympic-ro 43-gil, Songpa-gu, Seoul 138-736, Korea.
• Tel: (822) 3010-4377 • Fax: (822) 476-4719
• E-mail: medimash@gmail.com

INTRODUCTION

Ewing sarcoma is a malignant small round-cell tumor of the bone and soft tissue (1). In the past, classical skeletal Ewing sarcoma, extraskeletal Ewing sarcoma, primitive neuroectodermal tumor, and Askin tumor were classified as distinct pathological entities with variable degrees of neural differentiation. With recent advances in molecular diagnostics, it has become clear that these tumors are identical as they are derived from the same neuroectodermal cells and have non-random chromosomal translocations involving chromosome 22 and the Ewing sarcoma breakpoint region 1 gene (2). Currently, these tumors are referred to as

the Ewing sarcoma family of tumors (ESFTs), and the terms "peripheral primitive neuroectodermal tumor" and "Askin tumor" are no longer used (3).

Although ESFTs were traditionally considered an osseous-based sarcoma occurring in children and adolescents (1, 4), ESFTs can occur anywhere in the body (from head to toe) (3). Extraskeletal ESFTs (hereafter referred to as EES) are more common than skeletal Ewing sarcoma, particularly in adults (5, 6).

Ewing sarcoma family of tumors have attracted the interest of medical, surgical, and radiation oncologists as the combination of definitive local control, i.e., surgery and/or radiation therapy, and neoadjuvant/adjuvant chemotherapy greatly improves the prognosis of patients with ESFTs (5, 6). The initial comprehensive imaging evaluation of tumor status is extremely important to correctly guide the next management steps; thus, the current National Comprehensive Cancer Network and the European Society for Medical Oncology guidelines emphasize a multidisciplinary team approach for managing ESFTs (7, 8). In particular, diagnosis and management of EES arising in the head and neck, torso, and paravertebral region is more complex than those of skeletal Ewing sarcoma arising in the extremities; thus, warranting a truly multidisciplinary team approach.

Understanding the imaging features of primary EES as well as its metastatic patterns is important for radiologists who constitute an important part of the multidisciplinary team (4). However, radiologists may not be familiar with ESFTs of extraskeletal origin due to their rarity. Only a few articles have explored the imaging findings of EES in adults and its systematically metastatic pattern, which reveals that EES can manifest anywhere in the body as large masses (3, 4, 9). However, most prior studies were case series with a small number of patients or were case reports. Therefore, we intended to comprehensively analyze the spectrum of EES imaging features in adults and the metastatic pattern in a large series.

MATERIALS AND METHODS

Patients

Our Institutional Review Board approved this retrospective study and waived the requirement for informed consent. We performed a systematic computerized search of our hospital's database (Asan Biomedical Research Environment) from January 1996 to December 2013, using the diagnostic codes for "Ewing sarcoma", "primitive neuroectodermal

tumor", and "Askin tumor" as well as the demographic code for age ≥ 18 years. Using this search strategy, we identified 94 patients initially diagnosed with ESFT. We then manually selected patients using the following inclusion criteria: 1) diagnosis of ESFT was made based on biopsy or surgical specimens using fluorescence *in situ* hybridization (FISH) and/or polymerase chain reaction (PCR); 2) initial diagnosis was made at age ≥ 18 years; 3) images of primary or metastatic ESFTs were available; and 4) primary ESFT tumors originated from extraskeletal origin and without involvement of bone marrow or cortex on all available information including magnetic resonance imaging (MRI), computed tomography (CT), positron emission tomography/computed tomography (PET/CT), bone scans, and histology. Among the 94 patients, we excluded 24 patients as follows: 12 with age of onset < 18 years; and 12 with primary ESFT involving the skeleton. Therefore, 70 adults with EES were finally included in our study.

Image Acquisition

During the patient selection period, i.e., 17 years, various CT, MRI, and PET/CT scanners were used at our hospital. All 70 study patients underwent CT imaging of the chest and abdomen/pelvis as part of the initial evaluation. Flurodeoxyglucose (FDG)-PET/CT was obtained in 41 patients. MRI was usually performed (37 patients) if tumors occurred in the extremities, paravertebral region, or in the head and neck. No appropriate contrast-enhanced CT or MRI images of the primary tumors were available for 13 patients with initial metastatic disease who were referred to our hospital for chemotherapy after primary resection in the extremities. Although there were radiological reports with tumor descriptions for those 13 patients, we excluded them from the primary tumor imaging analysis. Therefore, the primary tumor imaging findings were evaluated in 57 patients.

Image Analysis

All available CT, MRI, and PET/CT scans obtained at the time of the initial diagnosis were reviewed retrospectively by consensus of two radiologists who specialize in abdominal radiology and with 6 and 8 years of clinical experience, respectively.

The primary tumor imaging features were qualitatively described in each organ. The images were specifically evaluated for lesion location, size, enhancement characteristics (homogenous or heterogeneous), presence of necrosis, margin (infiltrative or well-defined), invasion

of an adjacent organ, and distant metastases. If there was uniformly enhancing tissue in > 90% of the tumor, it was categorized as homogeneous enhancement. If the well-enhanced and less-enhanced portions were mixed, it was categorized as heterogeneous enhancement. If there was a non-enhanced portion in the center of the tumor, we regarded it as necrosis. The tumor margin was divided into two categories. A well-defined margin was defined as a smooth or lobulating margin without spiculation or infiltration into > 75% of the tumor perimeter. A poorly defined margin was defined as spiculation or infiltration into > 25% of the tumor perimeter. Invasion of adjacent organs was defined when the primary tumor directly engulfed or infiltrated into adjacent organs with obscuring the fat plane between the tumor and adjacent organs. Signal intensity (SI) of the tumor on T1- and T2-weighted images was evaluated in 37 patients who underwent MRI.

The distribution and imaging findings of metastatic tumors at the initial presentation were described for each organ. Metastatic sites were confirmed histologically by biopsy or were diagnosed as metastatic if they showed high FDG avidity on PET/CT scans as well as the typical metastasis findings on CT or MRI scans. We adopted the following criteria for lymph node metastases: 1) > 1.5 cm in short diameter; 2) lymph nodes containing a necrotic portion; 3) high FDG avidity on PET/CT; and 4) histological confirmation by biopsy.

RESULTS

Patients

Among the 70 patients included in our study, 29 were females (41.4%), and 41 were males (59.6%). Their mean age was 35.8 ± 15.6 years (range, 18–67 years). Of the 70 patients, 41 had locoregional disease and 29 had metastatic diseases at the initial presentation. Of the 70 patients, 20 (28.5%) had primary tumors in soft tissue and extremities, 18 (25.7%) in the abdomen and pelvis, 14 (20.0%) in the thorax, eight (11.4%) in the paravertebral space, and six (8.5%) in the head and neck. Four (5.7%) had widespread tumors that were histologically confirmed as Ewing sarcoma, but it was difficult to identify their primary sites (Table 1).

Imaging Features of the Primary Tumors

The imaging features of primary tumors of EES on contrast-enhanced CT or MRI were generally characterized as bulky heterogeneous masses with frequent local invasion or a mass effect to adjacent organs. Indeed, the mean largest tumor dimension was 9.1 cm (range, 1.3–23.0 cm). The majority of tumors showed heterogeneous enhancement (n = 42, 73.7%). Necrotic foci were observed in 41 patients (71.9%). Although these tumors generally showed a relatively well-defined margin (n = 38, 66.7%), local invasion to adjacent organs was also commonly observed (n = 26, 45.6%). In particular, local invasion was commonly noted in tumors of the abdomen (n = 6), pelvis (n = 4), and thorax (n = 8).

Nineteen tumors showed low SI on T1-weighted MRI (n = 37), and 18 tumors showed iso-SI compared to that of muscle. All tumors showed high T2-weighted SI that was either homogeneous (n = 9) or heterogeneous (n = 28).

The imaging features of the primary tumors of EES varied according to organ or tissue (Table 1). EESs in soft tissues and the extremities were intra- or inter-muscular masses

Table 1. Imaging Features of Primary Tumors of Extraskeletal Ewing Sarcoma Family of Tumors According to Primary Sites

Sites	Patient Number (%)	Imaging Features
Soft tissue and extremity	20 (28.6)	Intra- or inter-muscular well-defined mass (n = 15) Well-defined mass involving subcutaneous area (n = 5)
Abdomen and pelvis	18 (25.7)	Large solitary retroperitoneal mass (n = 4) Bulky or infiltrative mass in omentum, mesentery, or mesocolon (n = 4) Bulky exophytic mass in stomach, kidney, uterus, and prostate gland (n = 10)
Thorax	14 (20.0)	Pleural-based tumor or pleural thickening (n = 4) Bulky mass involving chest wall, lung parenchyma, mediastinum, or heart (n = 10)
Paravertebral space	8 (11.4)	Intradural extramedullary mass (n = 4) Extradural mass with neural foraminal extension (n = 4)
Head and neck	6 (8.6)	Polypoid mass and/or mucosal wall thickening in paranasal sinuses and orophaynx (n = 4) Extraaxial well-defined mass with mass effect to brain parenchyma (n = 2)
Unknown primary	4 (5.7)	Widespread metastatic disease including lymph node metastases (n = 4)

in a lower extremity (n = 9), upper extremity (n = 6), and as soft-tissue masses in the subcutaneous or skin layer of the chest wall (n = 2), vulva (n = 1), forehead (n = 1), and abdominal wall (n = 1).

Primary abdominal and pelvic EES tumors appeared as large retroperitoneal masses (n = 4), as peritoneal masses in the omentum, small bowel mesentery, or mesocolon (n = 4), as bulky subepithelial masses in the stomach, mimicking a gastrointestinal stromal tumor (n = 4), as exophytic masses in the kidney, mimicking renal cell carcinoma (n = 3) (Fig. 1), and as a mass in the uterus (n = 1) and prostate gland (n = 2). Tumors in the thorax appeared as pleural-based tumors (n = 4) (Fig. 2), chest-wall masses (n = 4), pulmonary parenchymal masses (n = 4), a mediastinal mass (n = 1), and as a heart mass (n = 1). Eight patients had paravertebral-located masses (four in the cervical spine
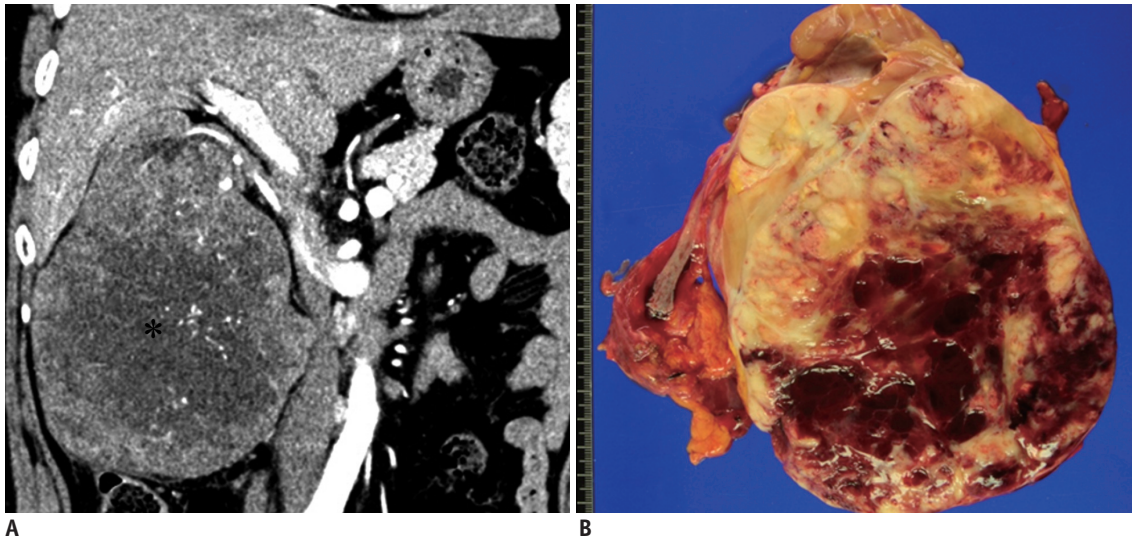
Fig. 1. 53-year-old woman with primary renal extraskeletal Ewing sarcoma family of tumors.
**A.** Coronal contrast-enhanced computed tomography scan of abdomen reveals large, heterogeneous, enhancing right renal mass with prominent internal vascular structure. Central, non-enhancing portions represent central tumor necrosis (asterisk). **B.** Gross pathological image from radical left nephrectomy demonstrates large mass in lower pole of kidney. Cut-surface shows pinkish yellow mass with internal hemorrhage and cystic change.
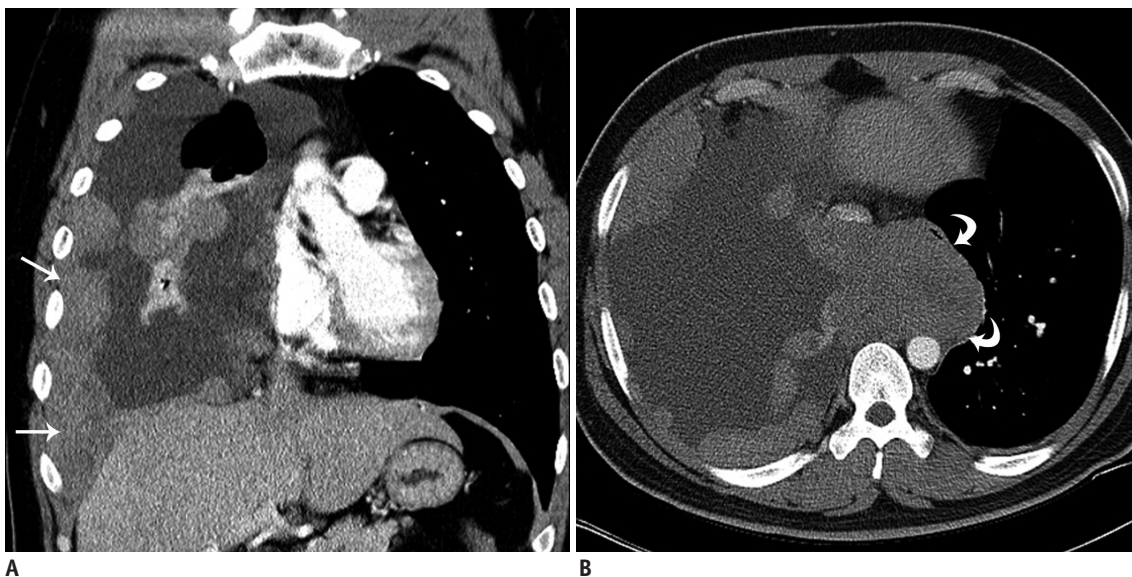
Fig. 2. 29-year-old man with thoracic extraskeletal Ewing sarcoma family of tumors.
A. Coronal contrast-enhanced computed tomography (CT) scan of chest shows multiple, pleural-based, enhancing masses (arrows) with large amount of pleural effusion. **B.** Axial contrast-enhanced CT scan shows bulky mediastinal mass in azygoesophageal recess, compressing esophagus and inferior vena cava (curved arrows).

and four in the sacrum), which manifested as intradural extramedullary or extradural masses with neural foraminal extension (Fig. 3). Of the six EESs in the head and neck, three were located in the paranasal sinuses, two were in the
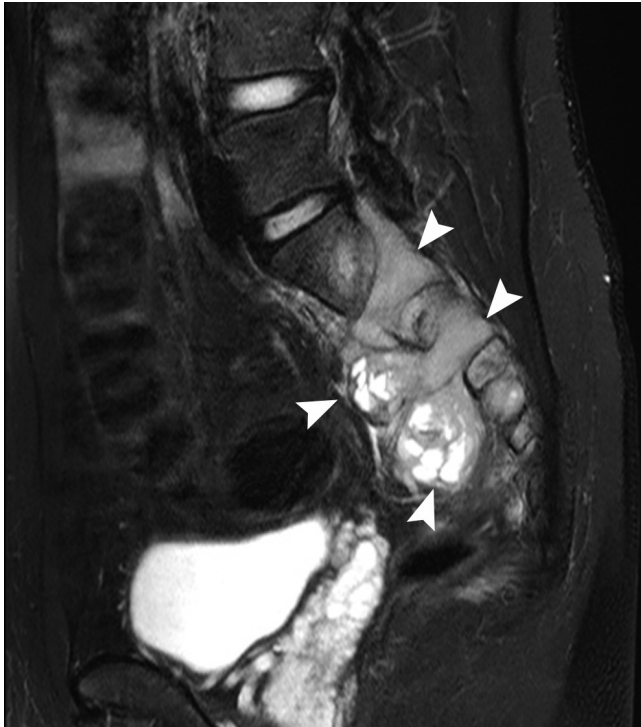
Fig. 3. 21-year-old man with paraspinal extraskeletal Ewing sarcoma family of tumors. Sagittal T2-weighted, fat-saturated magnetic resonance imaging scan shows hyperintense, dumbbell-shaped, extradural tumor left of S1–3. Tumor was connected to extraspinal component through neural foramen (arrowheads).

brain (Fig. 4), and one was in the oropharynx.

Metastatic Patterns of Extraskeletal Ewing Sarcoma

Notably, 29 patients had metastatic disease detected at one site at the initial diagnosis (n = 20, 69%), eight at two sites (n = 8, 28%), and one at multiple sites ≥ 3 (n = 1, 3%). The most frequent site of metastasis was a lymph node in 22 patients (75.9%), followed by bone (n = 9, 31.0%), lung (n = 6, 20.7%), abdominal solid organ (n = 4, 13.8%), peritoneum (n = 4, 13.8%), pleura (n = 2, 6.9%), and brain (n = 1, 3.4%) (Table 2). Most metastatic lesions in the 22 patients with an available PET/CT scan showed high FDG avidity with mean standardized uptake value maximum of 8.3 ± 3.9 (range, 2.0–18.0).

Lymph node metastases were identified in 22 patients ([histopathological confirmation; n = 7], [imaging diagnosis on both CT and PET; n = 15]) usually manifested as enlarged lymph nodes with or without internal necrosis in the mediastinum (n = 5), retroperitoneum (n = 8), internal and external iliac regions (n = 2), inguinal regions (n = 4), and cervical regions (n = 3) (Fig. 5). In 15 patients who underwent PET/CT, lymph node metastases always showed high FDG avidity. The lymph node metastasis was commonly found in patients with primary EESs of the torso, including the abdomen, lung, peritoneum, pleura, and paravertebral region (n = 18), compared to EESs in soft tissue and extremities, head, and neck (n = 4).

Distant bone metastases in nine patients showed FDG
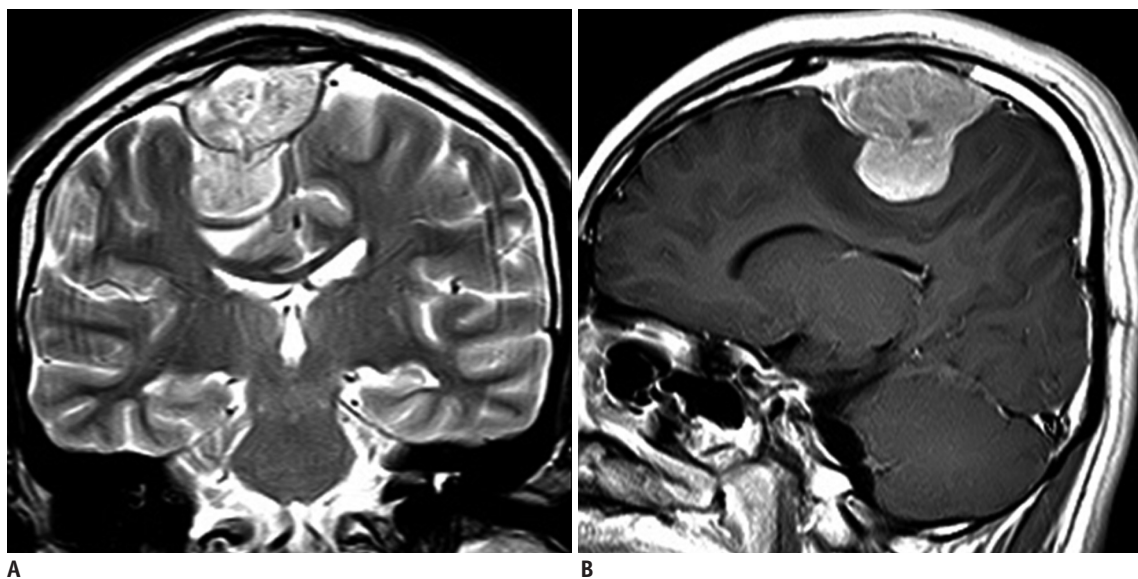
Fig. 4. 19-year-old man with primary extraaxial brain extraskeletal Ewing sarcoma family of tumors.
A. Coronal T2-weighted magnetic resonance imaging (MRI) scan shows hyperintense, dural-based mass in right frontal region. **B.** Sagittal post-gadolinium T1-weighted MRI scan shows intense contrast enhancement.

Table 2. Metastatic Patterns of Extraskeletal Ewing Sarcoma Family of Tumors

Sites	Patient Number (%)	Imaging Features
Lymph nodes	22 (75.9)	Enlarged lymph nodes in separate form or conglomerated form
Bone	9 (31.0)	Osteolytic bone tumors (n = 7) or diffuse bone metastases (n = 2)
Lung	6 (20.7)	Multiple lung nodules
Abdominal solid organs	4 (13.8)	Multiple hypodense nodules in liver (n = 2) Bulky bilateral adrenal masses (n = 2)
Peritoneum	4 (13.8)	Multiple, scattered, peritoneal nodules with ascites (n = 4)
Pleura	2 (6.9)	Bulky pleura-based masses (n = 4)
Brain	1 (3.4)	Multiple enhancing nodules in brain (n = 1)
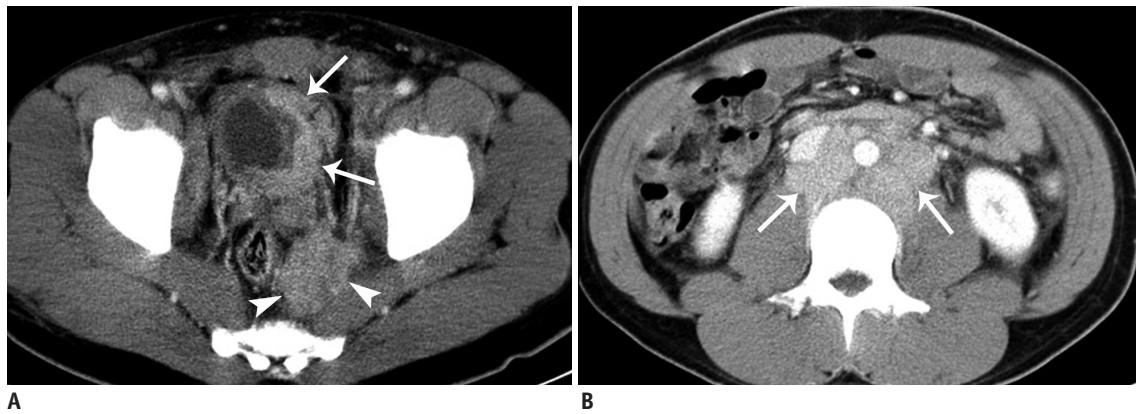
Fig. 5. 28-year-old man with lymph-node metastasis from pelvic extraskeletal Ewing sarcoma family of tumors.
A. Axial contrast-enhanced computed tomography (CT) scan shows perirectal, soft-tissue mass (arrowheads) invading left wall of bladder (arrows), which was proven to be Ewing sarcoma on biopsy. **B.** Axial contrast-enhanced CT scan shows conglomerated retroperitoneal lymphadenopathy (arrows).

avidity on the FDG-PET scan. Among the nine patients, CT/MRI showed destructive/osteolytic tumors in seven patients and diffuse bone metastases in two patients.

Liver metastases (n = 2) were seen as multiple, discrete, hepatic hypoattenuated nodules on the portal-venous phase of the contrast-enhanced CT scan. Metastases to adrenal glands (n = 2) were bilateral, bulky, adrenal masses with internal necrosis. Peritoneal metastases (n = 4) were seen as multiple, scattered, peritoneal nodules with ascites. Lung metastases were seen as multiple lung nodules (n = 6). Pleural metastases (n = 4) manifested as bulky, pleural masses. Brain metastases were seen in one patient as multiple, well-enhancing, discrete nodules in gray/white matter of the cerebral hemisphere and cerebellum.

DISCUSSION

In our series, the EESs occurred anywhere in the body from head to toe and mostly presented as bulky, soft-tissue masses with a mass effect to the adjacent tissue/organ. The spectrum of onset age of EESs in patients in our series was 18–67 years of age. These results generally agree with

observations that EESs usually occur in young adults, with a wide age of onset, and present as a large, heterogeneous mass in the trunk, extremities, or soft tissue (4). Notably, all patients included in our series were Asians, particularly Koreans, because a racial disparity in the incidence of Ewing sarcoma has been reported. According to one study that explored 1631 patients in North America, Caucasians have the highest occurrence of Ewing sarcoma (0.155), followed by Asians/Pacific Islanders (0.082), and African Americans (0.017) (10). Reported data are generally limited to Caucasians due to the low incidence and rarely concern Asians.

Clinical and radiological suspicion is important for diagnosing EES, as a conventional histological examination, i.e., hematoxylin-eosin staining, is limited to differentiating EES from other small, round, blue-cell tumors, such as metastatic neuroblastoma, lymphoma, or other soft-tissue sarcomas. A FISH cytogenetic evaluation is required to identify chromosomal translocations to confirm the EES diagnosis (11). However, FISH is not highly sensitive; thus, sequencing or PCR is recommended as an additional test if clinical/radiological suspicion is high (1, 8). Therefore, a

radiologist's suspicion of EES can be very helpful for making efficient diagnostic steps.

Although the imaging features of EES are non-specific, some clues suggest the possibility of EES in the differential diagnosis. For example, if bulky, pleural-based, soft-tissue masses with invasion of adjacent ribs and associated pleural effusion are present, the differential diagnosis should include EES, lung cancer, lymphoma, and other soft-tissue sarcomas. If paravertebral masses with ingrowth into the neural foramen or spinal canal are large and heterogeneous, EES should be considered with neurogenic tumors, such as schwannoma, neurofibroma, and malignant peripheral nerve-sheath tumor. EESs of the retroperitoneum and peritoneum are generally indistinguishable from other soft-tissue sarcomas, although EESs tend to displace and invade adjacent organs.

Interestingly, the metastatic pattern of our series differed somewhat from that seen in previous studies. According to previous studies, the lung is the most common metastatic site followed by bone, occurring in up to 80% and 40% of these patients, respectively, and lymph nodes are an uncommon metastatic site (4, 9, 12, 13). An analysis of the Surveillance, Epidemiology, and End Results database between 1973 and 2008 revealed that the incidence of regional lymph-node metastases is 12.4% for patients with EES (14). In contrast, lymph nodes were the most common site of metastases in our series (21/29, 71.4%), even though we adopted conservative criteria.

A possible explanation for the lymph node metastasis discrepancy may be different diagnostic criteria. The lymph node metastasis diagnosis was made by biopsy in seven patients and by imaging criteria in 15 patients in our study, whereas the previous studies usually used histological diagnosis for lymph node metastasis. However, we used strict imaging criteria for lymph node metastasis in our study, and cases with apparent lymph-node metastases were counted while excluding all indeterminate cases.

In addition, most patients with lymph node metastases had primary tumors in the torso, and we used extensive imaging studies to identify the metastatic disease, which may partly explain why lymph node metastasis was so common in our series. Indeed, Applebaum et al. (14) found that the incidence of EES with regional node involvement has consistently increased, particularly in recent years, likely reflecting that advances in imaging technology have improved detection. Perhaps, the racial difference between Caucasian and Asian patients may also be a factor

warranting further investigation.

Our study had several limitations. First, the sample size was relatively small. However, the incidence of Ewing sarcoma is remarkably lower in Asians than that in Caucasians, and < 40 new cases are detected annually in South Korea (15). Therefore, studies regarding Ewing sarcoma in Asia have been confined to small case series or case reports. Our study is the largest series conducted in Asia. Second, we may have had a referral bias in our study population, as patients who are referred to our sarcoma center often have advanced disease. This referral bias could explain the higher incidence of metastases in our series. Third, we have used various CT, MRI and PET scanners, and have used various contrast agents. However, we adopted standard imaging protocols in all of the scanners used in our institution; thus; the qualitative assessment of tumor characteristics may not have been affected by using different scanners. These limitations could not be avoided, as this was a retrospective study.

In summary, we present a wide spectrum of imaging features and metastatic patterns of EES in adult Asian patients. Primary EES can occur anywhere from head to toe, and mostly manifests as a large and bulky soft-tissue mass. Lymph nodes were the most frequent site of metastases in our series, followed by lung, bone, solid organs, and peritoneum/pleura.

REFERENCES

1. Cote GM, Choy E. Update in treatment and targets in Ewing sarcoma. *Hematol Oncol Clin North Am* 2013;27:1007-1019
2. Jain S, Xu R, Prieto VG, Lee P. Molecular classification of soft tissue sarcomas and its clinical applications. *Int J Clin Exp Pathol* 2010;3:416-428
3. Murphey MD, Senchak LT, Mambalam PK, Logie CI, Klassen-Fischer MK, Kransdorf MJ. From the radiologic pathology archives: ewing sarcoma family of tumors: radiologic-pathologic correlation. *Radiographics* 2013;33:803-831
4. Javery O, Krajewski K, O'Regan K, Kis B, Giardino A, Jagannathan J, et al. A to Z of extraskeletal Ewing sarcoma family of tumors in adults: imaging features of primary disease, metastatic patterns, and treatment responses. *AJR Am J Roentgenol* 2011;197:W1015-W1022
5. Krasin MJ, Davidoff AM, Rodriguez-Galindo C, Billups CA, Fuller CE, Neel MD, et al. Definitive surgery and multiagent systemic therapy for patients with localized Ewing sarcoma family of tumors: local outcome and prognostic factors. *Cancer* 2005;104:367-373
6. Womer RB, West DC, Krailo MD, Dickman PS, Pawel BR, Grier HE, et al. Randomized controlled trial of interval-compressed

chemotherapy for the treatment of localized Ewing sarcoma: a report from the Children's Oncology Group. *J Clin Oncol* 2012;30:4148-4154

7. von Mehren M, Randall RL, Benjamin RS, Boles S, Bui MM, Casper ES, et al. Soft tissue sarcoma, version 2.2014. *J Natl Compr Canc Netw* 2014;12:473-483

8. Paulussen M, Bielack S, Jürgens H, Casali PG; ESMO Guidelines Working Group. Ewing's sarcoma of the bone: ESMO clinical recommendations for diagnosis, treatment and follow-up. *Ann Oncol* 2009;20 Suppl 4:140-142

9. Somarouthu BS, Shinagare AB, Rosenthal MH, Tirumani H, Hornick JL, Ramaiya NH, et al. Multimodality imaging features, metastatic pattern and clinical outcome in adult extraskeletal Ewing sarcoma: experience in 26 patients. *Br J Radiol* 2014;87:20140123

10. Jawad MU, Cheung MC, Min ES, Schneiderbauer MM, Koniaris LG, Scully SP. Ewing sarcoma demonstrates racial disparities in incidence-related and sex-related differences in outcome: an analysis of 1631 cases from the SEER database, 1973-2005. *Cancer* 2009;115:3526-3536

11. Kumar S, Pack S, Kumar D, Walker R, Quezado M, Zhuang Z, et al. Detection of EWS-FLI-1 fusion in Ewing's sarcoma/peripheral primitive neuroectodermal tumor by fluorescence in situ hybridization using formalin-fixed paraffin-embedded tissue. *Hum Pathol* 1999;30:324-330

12. Bernstein M, Kovar H, Paulussen M, Randall RL, Schuck A, Teot LA, et al. Ewing's sarcoma family of tumors: current management. *Oncologist* 2006;11:503-519

13. El Weshi A, Allam A, Ajarim D, Al Dayel F, Pant R, Bazarbashi S, et al. Extraskeletal Ewing's sarcoma family of tumours in adults: analysis of 57 patients from a single institution. *Clin Oncol (R Coll Radiol)* 2010;22:374-381

14. Applebaum MA, Goldsby R, Neuhaus J, DuBois SG. Clinical features and outcomes in patients with Ewing sarcoma and regional lymph node involvement. *Pediatr Blood Cancer* 2012;59:617-620

15. Lee JA, Kim DH, Cho J, Lim JS, Koh JS, Yoo JY, et al. Treatment outcome of Korean patients with localized Ewing sarcoma family of tumors: a single institution experience. *Jpn J Clin Oncol* 2011;41:776-782